

# A Highly Sensitive and Selective Fluorescent Sensor for Detection of Al<sup>3+</sup> Using a Europium(III) Quinolinecarboxylate

Wentao Xu,<sup>†</sup> Youfu Zhou,<sup>\*,†</sup> Decai Huang,<sup>†</sup> Mingyi Su,<sup>†,‡</sup> Kun Wang,<sup>†,‡</sup> and Maochun Hong<sup>†</sup>

<sup>†</sup>Key Laboratory of Optoelectronic Materials Chemistry and Physics, Fujian Institute of Research on the Structure of Matter, Chinese Academy of Sciences, Fuzhou 350002, China

<sup>‡</sup>University of the Chinese Academy of Sciences, Beijing 100049, China

## Supporting Information

**ABSTRACT:** Eu<sub>2</sub>PQC<sub>6</sub> has been developed to detect Al<sup>3+</sup> by monitoring the quenching of the europium-based emission, with the lowest detection limit of ~32 pM and the quantitative detection range to 150 μM. Eu<sub>2</sub>PQC<sub>6</sub> is the first ever example that the europium(III) complex serves as an Al<sup>3+</sup> fluorescent sensor based on “competition-displacement” mode.

As the most abundant metallic element in the earth's crust, aluminum is widely used in modern society, such as light alloys, pharmaceuticals, and water purification.<sup>1</sup> Aluminum in daily life is ubiquitous; however, environmental acidification increases the amount of free Al<sup>3+</sup> ions, leading to accumulation, which is deadly to plant roots and humans.<sup>2</sup> The World Health Organization recommends that the tolerable weekly dietary human intake of aluminum is 7 mg kg<sup>-1</sup> body weight.<sup>3</sup> Excess aluminum results in toxicological effects, causing Alzheimer's disease, Parkinsonism dementia, osteoporosis, colic, and rickets.<sup>4</sup> Facile detection of Al<sup>3+</sup> is therefore vital in environmental and biological research. At present, the main detection methods, like atomic absorption and inductively coupled plasma atomic emission spectrometry, are complicated and expensive.

Recently, the design of a heavy-metal-ion sensor based on fluorophore is active because of its operational simplicity, instantaneous response, and nondestructive character.<sup>5</sup> However, most of these substances require complicated syntheses and cannot surmount their limitations, like short fluorescent lifetime, narrow energy gap, and interference of Fe<sup>3+</sup> and Cu<sup>2+</sup>.<sup>6</sup> So, the Al<sup>3+</sup> sensor with improved properties is still in high demand. Major research interest has focused on the lanthanide complex, taking advantage of analyte-induced energy transfer or changes of the coordination environment. Because of high luminous efficiency and long-wavelength emission and lifetime, lanthanide complexes have the potential for application, offering considerable virtues over typical fluorophore sensors.<sup>7</sup> Some europium(III), terbium(III), and ytterbium(III) systems have been synthesized for detection of Zn<sup>2+</sup> and Hg<sup>2+</sup>.<sup>7b,c</sup> However, to the best of our knowledge, there is still not an Al<sup>3+</sup> sensor based on the lanthanide complex. Herein, we designed and synthesized a binary europium complex, Eu<sub>2</sub>PQC<sub>6</sub>, where PQC has been proven to be a valuable antenna for sensitizing Eu<sup>III</sup> emission.<sup>8</sup> Meanwhile, the coordination between the carboxyl group of PQC and Eu<sup>III</sup> should be disturbed in solution by other metal ions like Al<sup>3+</sup>,

which is the hardest acid among all of the cations.<sup>9</sup> The stronger coordination ability between the ligand and Al<sup>3+</sup> can lead to decomposition of the europium complex. On the basis of this “competition-displacement” mode, the Al<sup>3+</sup>-induced change of the coordination environment is expected to modulate the Eu<sup>III</sup> emission. Moreover, this binary system using PQC as an antenna- and analyte-identified group simultaneously is more efficient and facile than the trinary example.<sup>7b</sup>

By solvothermal reaction, Eu<sub>2</sub>PQC<sub>6</sub> can be prepared in high yield. A structural investigation reveals that, in the asymmetric unit, each Eu<sup>III</sup> center is coordinated by nine oxygen atoms from three PQC ligands and two terminal ethanol (EtOH) molecules (Figure S1 in the Supporting Information, SI). Eu<sub>2</sub>PQC<sub>6</sub> features a discrete dinuclear structure joined by two carboxyl groups to form a twisty rectangular platelike unit. The coordination geometry can be described as a distorted tricapped trigonal prism, and the PQC ligands exhibit chelate and bridge coordination modes (Figure 1). The dinuclear unit is further

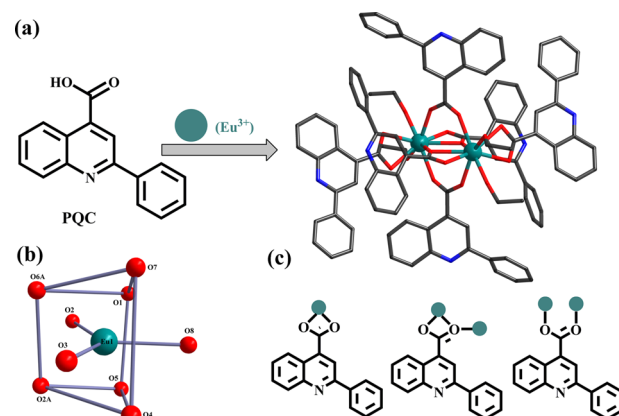


**Figure 1.** (a) Structure views of PQC and Eu<sub>2</sub>PQC<sub>6</sub>. (b) Coordination polyhedron of the Eu<sup>III</sup> ion. (c) Coordination modes of PQC.

connected by four adjacent ones to form a 3D supramolecular framework through  $\pi\cdots\pi$  interactions (Figure S2 in the SI). The dinuclear formation in ethanol has been confirmed by electrospray ionization mass spectrometry (ESI-MS) with a peak at  $m/z$  1070.6, assignable to  $[\text{Eu}_2\text{PQC}_6 + 4\text{H}_2\text{O}]/2$  (calcd  $m/z$  1070.9; Figure S20 in the SI).

Received: April 30, 2014

Published: June 23, 2014

The absorption spectra of  $\text{Eu}_2\text{PQC}_6$  and PQC ( $5 \mu\text{M}$ ) are monitored in a 95:5 (v/v) EtOH–dimethyl sulfoxide (DMSO) solution, consisting of two distinguishable bands at 262 and 330 nm, attributed to the  $\pi \rightarrow \pi^*$  and  $n \rightarrow \pi^*$  transitions of PQC. Upon the addition of  $\text{Al}^{3+}$ , the profiles of both transition bands change progressively and are red-shifted to 265 and 339 nm, respectively (Figures S3 and S4 in the SI). The absorbance changes versus the molar fraction of  $\text{Al}^{3+}$  suggest that the most significant interaction occurs at 3.0 equiv of  $\text{Al}^{3+}$ . These changes can be viewed as a successful displacement of  $\text{Eu}^{\text{III}}$  from PQC, simultaneously accommodated with  $\text{Al}^{3+}$ , indicating the formation of Al-PQC with 1:2 stoichiometry.

The emission spectra of  $\text{Eu}_2\text{PQC}_6$  in solution in the absence and presence of  $\text{Al}^{3+}$  ions are also monitored (Figure 2). Under

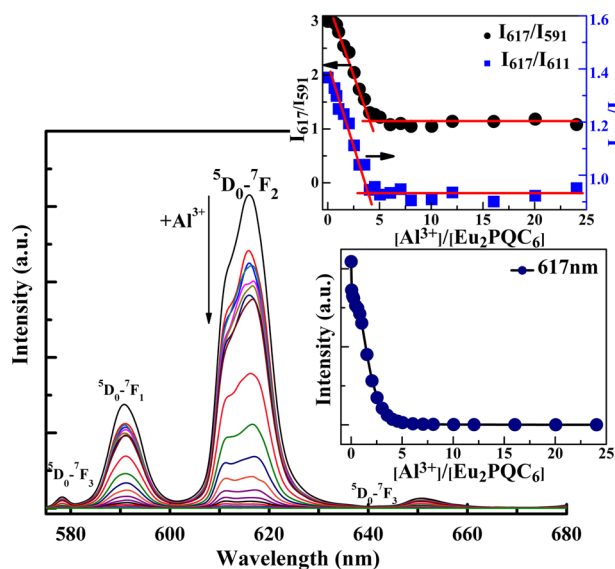


**Figure 2.** Changes in the  $\text{Eu}^{\text{III}}$  emission of  $\text{Eu}_2\text{PQC}_6$  in a 95:5 (v/v) EtOH–DMSO solution upon the addition of  $\text{Al}^{3+}$  (0–24 equiv). Inset: changes in the ratio of  $I_{617}/I_{591}$ ,  $I_{617}/I_{611}$ , and  $I_{617}$  of  $\text{Eu}^{\text{III}}$  emission versus equiv of  $\text{Al}^{3+}$  added.

excitation at 330 nm, the characteristic emission peaks of  $\text{Eu}^{\text{III}}$  at 579, 591, 617, and 650 nm assigned to the  $^5\text{D}_0 \rightarrow ^7\text{F}_J$  ( $J = 0, 1, 2, 3$ ) transitions appear. Upon the addition of  $\text{Al}^{3+}$ , the intensity of the maximum band at 617 nm decreases significantly, resulting in 93.1% and 99.4% quenching after titration of 3.0 and 6.0 equiv of  $\text{Al}^{3+}$ , along with the lifetime and quantum yield changing from 0.91 ms and 18.71% to 0.68  $\mu\text{s}$  and 0.52% (Figure S5 in the SI). A major advantage for this europium sensor is the incorporation of a ratiometric, where the magnetic dipole-induced  $J = 1$  transition is relatively insensitive to changes in coordination whereas the  $J = 2$  transition is hypersensitive.  $\text{Al}^{3+}$  shows distinct behavior with peak splitting at the  $J = 2$  transition (a new band at 611 nm) and a remarkable decrease for the ratio of  $I_{617}/I_{591}$  and  $I_{617}/I_{611}$  from 3.0 to 1.3 and from 1.4 to 1.0, respectively, which reflect perturbation in the coordination environment of  $\text{Eu}^{\text{III}}$ . Analysis of these changes as a function of added  $\text{Al}^{3+}$  is shown as an inset in Figure 2. The changes in all cases decrease significantly before reaching a plateau at about 3.0 equiv of  $\text{Al}^{3+}$ , demonstrating again that  $\text{Eu}_2\text{PQC}_6$  interacts with added ions in a 1:3 stoichiometry (Al:PQC = 1:2). So, the quenching mechanism here involves the  $\text{Al}^{3+}$ -induced displacement of  $\text{Eu}^{\text{III}}$  with concomitant formation of Al-PQC<sub>2</sub>. The absence of any change (apart from a loss in intensity) in the excitation spectra and the appearance of a peak

at 390 nm similar to PQC-based emission, corresponding to the mirror image of the quenching seen in the red region, corroborates this fact (Figures S6–S8 in the SI).

From this replacement assay, the response parameter  $\alpha$ , defined as the ratio of the nondisplaced  $\text{Eu}_2\text{PQC}_6$  concentration to the initial concentration, is plotted as a function of  $\text{Al}^{3+}$ , and the binding constant for the formation of Al-PQC<sub>2</sub> as  $\log K_b = 13.2$  has been calculated from a double-logarithmic regression equation. The limit of detection (LOD) is determined as 32.2 pM for  $\text{Al}^{3+}$  by monitoring the sensitive  $\text{Eu}^{\text{III}}$  emission, which has achieved the lowest level compared with the data reported (Figures S9–S11 in the SI).<sup>5</sup> The LOD is orders of magnitude lower than the organic probes (from micromolar to picomolar), and the linear proportional extends to the range of 150  $\mu\text{M}$ , so this sensor has potential application in trace analysis. Furthermore, the quick response of this probe to  $\text{Al}^{3+}$ , owing to the fast displacement process, provides a “zero-wait” detection method (Figure S12 in the SI). In addition, luminescence in the presence of 500-fold concentration of acetic acid and triethylamine has been detected, in which  $\text{Eu}_2\text{PQC}_6$  maintains 31% and 48% intensity, respectively, and the ratio of  $I_{617}/I_{591}$  remains at about 3.0 (Figure S13 in the SI).

To better understand the interaction mode between  $\text{Eu}_2\text{PQC}_6$  and  $\text{Al}^{3+}$ , the  $^1\text{H}$  NMR titrations of  $\text{Al}^{3+}$  with PQC and  $\text{Eu}_2\text{PQC}_6$  are recorded in DMSO-*d*<sub>6</sub>. Upon the addition of 0.5 equiv of  $\text{Al}^{3+}$  to PQC, the signal at  $\delta$  14.00 disappears, indicating deprotonation of the carboxyl group during complexation, which strongly suggests the direct involvement of the COOH group for  $\text{Al}^{3+}$  chelation. The C–H signal ( $\delta$  8.67–7.52) of the rings shows a slight upfield shift to  $\delta$  8.65–7.50 (Figure S14 in the SI). Although the extent of the shift is small, it stays within the range observed by other workers for the indirect binding group of the ligand.<sup>10</sup> Upon the addition of  $\text{Al}^{3+}$  to a  $\text{Eu}_2\text{PQC}_6$  solution, significant spectral changes are observed with 3.0 equiv of  $\text{Al}^{3+}$ ; excess additions do not affect the spectra virtually (Figure 3). The C–H signals are shifted upfield by  $\delta$  0.23–0.38, and the final pattern agrees well with the Al-PQC titration spectra. This observation indicates that the original coordination between PQC and  $\text{Eu}^{\text{III}}$  has been interrupted by  $\text{Al}^{3+}$  to form a new

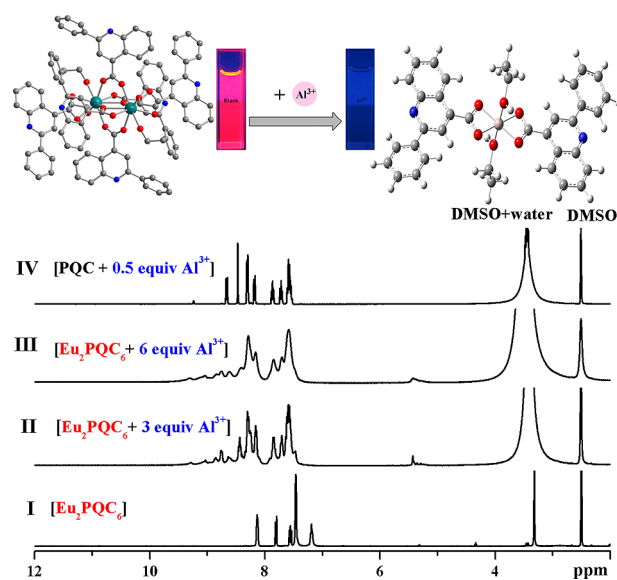


**Figure 3.** Binding mode of Al-PQC<sub>2</sub> and  $^1\text{H}$  NMR spectra of  $\text{Eu}_2\text{PQC}_6$  and PQC with  $\text{Al}(\text{NO}_3)_3$  in DMSO-*d*<sub>6</sub>.

complex. The mass spectrum also confirms the 1:2 binding stoichiometry of  $\text{Al}^{3+}$  with PQC. Upon the addition of 3.0 equiv of  $\text{Al}^{3+}$  to  $\text{Eu}_2\text{PQC}_6$ , the intense peak at  $m/z$  319.0 (Figure S21 in the SI) corresponding to  $[\text{Al}(\text{PQC})_2(\text{EtOH})_2 + \text{Na}^+]/2$  (calcd  $m/z$  319.2) is observed. From the results of fluorescence,  $^1\text{H}$  NMR, and ESI-MS data titration, we induce that the evolution of  $\text{Eu}_2\text{PQC}_6$  should be attributed to the coordination ability and acidity of  $\text{Al}^{3+}$ , and the  $\text{Al-PQC}_2$  formed in solution can be determined. The proposed structure of  $\text{Al-PQC}_2$  optimized by density functional theory (DFT) calculations (Figure S15 in the SI) indicates an octahedral geometry, where the equatorial and axial positions are occupied by six oxygen atoms from PQC and EtOH, respectively. The donation of the lone electron pairs of oxygen to  $\text{Al}^{3+}$  leads to a high energetic stabilization, with a total energy of  $-2194.45605$  au.

To establish the selectivity of  $\text{Eu}_2\text{PQC}_6$  for  $\text{Al}^{3+}$ , the effect of competing metal ions ( $\text{Li}^+$ ,  $\text{Na}^+$ ,  $\text{K}^+$ ,  $\text{Mg}^{2+}$ ,  $\text{Ca}^{2+}$ ,  $\text{Mn}^{2+}$ ,  $\text{Fe}^{2+}$ ,  $\text{Fe}^{3+}$ ,  $\text{Co}^{2+}$ ,  $\text{Ni}^{2+}$ ,  $\text{Cu}^{2+}$ ,  $\text{Zn}^{2+}$ , and  $\text{Cd}^{2+}$ ) is investigated. For this purpose,  $\text{Eu}_2\text{PQC}_6$  is treated with 3.0 equiv of  $\text{Al}^{3+}$  in the presence of other ions (6.0 equiv). The overall changes observed in the  $\text{Eu}^{\text{III}}$  emission (617 nm) are presented (Figure S16 in the SI), indicating that the luminescence is slightly influenced by most cations, while  $\text{Cu}^{2+}$  and  $\text{Fe}^{3+}$  are somewhat quenched but clearly detectable. The significant distinction in fluorescence between  $\text{Al}^{3+}$  and the other ions guarantees the low interference for detection. Like our predictions, this unique selectivity can be interpreted in terms of the coordination ability between the metal ion and PQC. We calculate the interaction energies between the selected cations and PQC based on the DFT method at the B3LYP/6-31G\* level (Table S3 and Figure S17 in the SI). It has been found, in line with the luminescent data, that PQC is the most strongly bonded to  $\text{Al}^{3+}$  (interaction energy:  $-486.11718$  kJ mol $^{-1}$ ), which is about 4 and 2 times that of the alkali- and transition-metal ions, respectively. The DFT method allows us to observe that it is indeed predominantly due to the lowest orbital interaction.

It is worth nothing that  $\text{Eu}_2\text{PQC}_6$  shows poor emission in a mixed aqueous solution (10% water leading to 64% quenching), which can be attributed to the coordination of  $\text{H}_2\text{O}$  to the  $\text{Eu}^{\text{III}}$  center (Figure S18 in the SI). The O–H oscillators trigger nonradiative scattering processes and reduce the quantum yield. The lifetimes at 617 nm, in 10% mixed  $\text{H}_2\text{O}$ –DMSO and  $\text{D}_2\text{O}$ –DMSO (10:90, v/v), have been recorded as  $\tau_{\text{H}_2\text{O}} = 0.57$  ms and  $\tau_{\text{D}_2\text{O}} = 1.15$  ms, respectively, from which the number of coordinated water molecules to each  $\text{Eu}^{\text{III}}$  center  $q = 0.77$  can be determined (Figure S19 in the SI). In the following work, we plan to use a second ligand like 2,2'-bipyridine to saturate the lanthanide ion, designing a probe with a hydrophobic aromatic shell.

In summary, we have developed, to the best of our knowledge, the first example of an europium complex for detection of  $\text{Al}^{3+}$ . The lowest LOD, long linear range, and anti-interference of  $\text{Fe}^{3+}/\text{Cu}^{2+}$  during recognition have been achieved. The sensitivity and selectivity have been investigated in detail. This luminescent-sensitive complex can be applied in trace analysis, and the “competition-displacement” concept can serve as a platform to design ion probes with differential selectivity. Further studies on the lanthanide complexes for detection in an aqueous solution are underway.

## ■ ASSOCIATED CONTENT

### 📄 Supporting Information

X-ray crystallographic data in CIF format, experimental details, additional structural spectra, analysis, and calculation. This material is available free of charge via the Internet at <http://pubs.acs.org>.

## ■ AUTHOR INFORMATION

### Corresponding Author

\*E-mail: [yfzhou@fjirsm.ac.cn](mailto:yfzhou@fjirsm.ac.cn).

### Notes

The authors declare no competing financial interest.

## ■ ACKNOWLEDGMENTS

The authors are grateful to the National Nature Science Foundation of China (Grants 91022035), Natural Science Funds of Fujian Province (Grant 2012H0047), and CAS Hundred Talents Program for financial support of this work.

## ■ REFERENCES

- (1) Verstraeten, S. V.; Aimo, L.; Oteiza, P. I. *Arch. Toxicol.* **2008**, *82*, 789–802.
- (2) Delhaize, E.; Ryan, P. R. *Plant Physiol.* **1995**, *107*, 315–321.
- (3) Barcelo, J.; Poschenrieder, C. *Environ. Exp. Bot.* **2002**, *48*, 75–92.
- (4) Wang, B.; Xing, W.; Zhao, Y.; Deng, X. *Environ. Toxicol. Pharmacol.* **2010**, *29*, 308–313.
- (5) (a) Sahana, A.; Banerjee, A.; Lohar, S.; Sarkar, B.; Mukhopadhyay, S. K. *Inorg. Chem.* **2013**, *52*, 3627–3633. (b) Maity, D.; Govindaraju, T. *Inorg. Chem.* **2010**, *49*, 7229–7231. (c) Li, Y.; Liu, X.; Zhang, Y.; Chang, Z. *Inorg. Chem. Commun.* **2013**, *33*, 6–9. (d) Li, Y.; Li, J.; Wang, L.; Zhou, B.; Chen, Q.; Bu, X. *J. Mater. Chem. A* **2013**, *1*, 495–499.
- (6) (a) Formica, M.; Fusi, V.; Giorgi, L.; Micheloni, M. *Coord. Chem. Rev.* **2012**, *256*, 170–192. (b) Ng, S. M.; Narayanaswamy, R. *Anal. Bioanal. Chem.* **2006**, *386*, 1235–1244.
- (7) (a) Liu, Z.; He, W.; Guo, Z. *Chem. Soc. Rev.* **2013**, *42*, 1568–1600. (b) Comby, S.; Tuck, S. A.; Truman, L. K.; Kotova, O.; Gunnlaugsson, T. *Inorg. Chem.* **2012**, *51*, 10158–10168. (c) Weitz, E. A.; Pierre, V. C. *Chem. Commun.* **2011**, *47*, 541–543.
- (8) (a) Xu, W.; Zhou, Y.; Huang, D.; Xiong, W.; Su, M.; Wang, K.; Han, S.; Hong, M. *Cryst. Growth Des.* **2013**, *13*, 5420–5432. (b) Gai, Y.; Xiong, K.; Chen, L.; Bu, Y.; Li, X.; Jiang, F.; Hong, M. *Inorg. Chem.* **2012**, *51*, 13128–13137.
- (9) Paar, R. G.; Pearson, R. G. *J. Am. Chem. Soc.* **1983**, *105*, 7512–7516.
- (10) Tiwari, K.; Mishra, M.; Singh, V. P. *RSC Adv.* **2013**, *3*, 12124–12132.